Rough interfaces in a bcc-based binary alloy

F. Schmid and K. Binder
Institut für Physik, Universität Mainz, Staudinger Weg 7, D-6500 Mainz, Federal Republic of Germany
(Received 3 April 1992)

The structure of antiphase domain boundaries in the ordered phase of body-centered-cubic alloys is investigated by Monte Carlo simulations, studying a fairly realistic model of iron-aluminum alloys that includes a description of the magnetic properties of iron within a nearest-neighbor Heisenberg Hamiltonian. An interface is enforced by employing in one lattice direction an odd number of lattice planes and choosing periodic boundary conditions throughout. At the temperatures of interest, the antiphase domain boundary is not localized in the system and is rough, which implies a logarithmic dependence of the interfacial width on the linear dimension $L_{\parallel}$ parallel to the interface. Methods are introduced to define an instantaneous interface position for each configuration that is analyzed. Choosing a coordinate frame whose origin is fixed at this (moving) interface position, profiles of order parameter, concentration, etc., can be estimated. It is found that capillary wave theory accounts for the interface widths reasonably well. Near the bulk critical temperature the lengths characterizing the intrinsic interfacial widths agree with the bulk correlation length, which is obtained from an independent investigation of correlation functions in the bulk. Finally, the interfacial enrichment of the majority species in the domain wall is studied and it is shown that the critical behavior of the interfacial excess concentration is consistent with scaling predictions.

I. INTRODUCTION

The study of interfaces in solids represents a topic of great importance in materials research as well as in statistical physics. From the theoretical point of view, one is interested in what happens if the translational symmetry of a system is broken in one direction. In materials research interfaces represent a large class of defects in crystals and thus determine many properties of these systems. Interfaces in solid systems have therefore been investigated by experiments very extensively[1] and there exist some theoretical concepts to describe them.[2] Yet theoretical studies of microscopic systems usually treat very simple model systems, such as, e.g., the Ising model with nearest-neighbor interaction. However, interfaces in more complex systems exhibit a variety of interesting phenomena. In alloys, for example, the effect of interfacial segregation has attracted considerable interest.[3,4] Usually, this effect is explained by the occurrence of mechanical strains and forces in the neighborhood of the interface, but still the question remains open to what extent segregation could already arise in a system without mechanical constraints. One might also be interested in the behavior of the interface near the disorder transition. Actually the evolution of an interface, if one approaches a line of first-order transitions, has recently been studied both experimentally and theoretically in a fcc-based alloy.[5,6] Among other things, we will present here a similar (theoretical) investigation for a line of second-order transitions.

In an earlier paper[7] we have introduced a model for a substitutional bcc-based binary alloy, particularly adapted to the system iron-aluminum. The model takes into consideration configurational (Ising) and magnetic (Heisenberg) degrees of freedom and its exchange interactions are directly based on the microscopic properties of iron-aluminum (short-range order). We showed that it in fact reproduces the iron-rich side of the iron-aluminum phase diagram in a topologically correct way. The knowledge of the bulk properties of this model enables us now to study interfaces in this complex model, which is moreover strongly related to a real system.

Our paper is organized as follows. First we define the model, describe our Monte Carlo method, and comment on some special finite size effects. In the next section we present a simple Landau theory and review some important features of the capillary wave approximation. Our simulation results are described in Sec. IV. We first concentrate on the length scales related to the interface, comparing them with the capillary wave theory and with the bulk correlation length. Furthermore, as already mentioned, we will take particular interest in the occurrence of interfacial segregation and in its evolution with temperature. We will also have a look at the scaling properties of other quantities near the transition. We summarize our results in Sec. V.

II. THE MODEL AND THE SIMULATION METHOD

Basically, our model is an Ising model on a bcc lattice. The Ising spins take the values $S_i = \pm 1$, modeling in this way a binary substitutional alloy (the Ising spin $+1$ stands for iron, the Ising spin -1 represents aluminum). Furthermore, sites with Ising spin $+1$ are supposed to have a magnetic moment, modeled by a classical Heisenberg spin ($|\sigma_i| = 1$). In the grand canonical ensemble, the Hamiltonian of this model is given by

$$\mathcal{H}=-\tfrac{1}{2}\sum_{i\neq j}V_{ij}S_iS_j-\tfrac{1}{2}\sum_{i\neq j}J_{ij}\frac{1+S_i}{2}\frac{1+S_j}{2}\sigma_i\sigma_j - H\sum_i S_i\ , \tag{1}$$

where H is related to the chemical potential difference between the two species and the exchange interactions V_{ij} and J are chosen to be $V_1=-12$ meV, $V_2/|V_1|=-0.167$, $V_3/|V_1|=0.208$, $J_1/|V_1|=1.65$ (see Refs. 7 and 8). The notation V_μ refers to site j being the μth coordination shell of site i. Thus the crystallographic interactions extend to third nearest neighbors, while only nearest-neighbor interaction is taken into account. Figure 1 shows the bulk phase diagram in the grand canonical ensemble.

Within this model, we have studied a (100) antiphase boundary in the ordered $B2$ phase (see Fig. 2). Therefore we considered rectangular systems of body-centered-cubic lattices with periodic boundary conditions in all directions and linear dimensions $L_\perp\times L_\parallel\times L_\parallel$. To produce the interface, we chose the number of layers $L_\perp$ in the x direction to be odd. Hence the interface is not pinned to a particular position, it can wander and one has translational invariance (Fig. 3). To be able to study profile properties like profile widths, interface segregation, etc., one has to localize the interface in each configuration separately.

We used two different ways of doing this: To begin with we note that the periodic boundary conditions define a periodic continuation

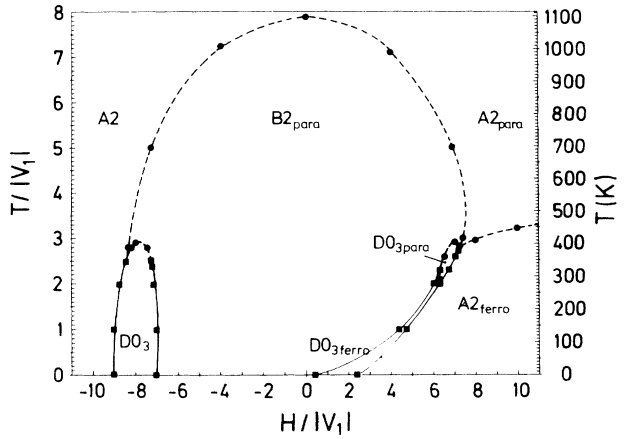

FIG. 1. Bulk phase diagram of our model in the grand canonical ensemble. $A2$ denotes the crystallographically disordered structure of the bcc alloy. In the $B2$ structure the lattice is split into two simple cubic sublattices, one taken preferentially by the A atoms and the other by the B atoms of the binary (AB) alloy. In the DO_3 phase the lattice splits into four face-centered-cubic sublattices, one of which is occupied preferentially by B atoms while the three others are occupied preferentially by A atoms. $A2$ and DO_3 phases occur both in ferro- and in paramagnetic states. Second-order transitions are shown as broken curves, while full curves denote first-order transitions. In the present work only $H/|V_1|=4$ is considered at $T/|V_1|\geq 1.5$ (from Ref. 7).

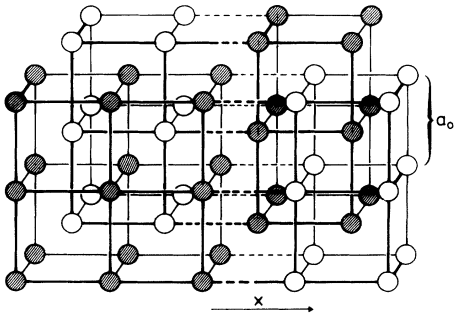

FIG. 2. An antiphase boundary in (100) direction in the ordered $B2$ phase. If one subdivides the bcc lattice in two simple cubic lattices a and b, the order parameter of the $B2$ phase can be defined as $M=c_A(a)-c_A(b)$. At the interface two $B2$ domains displaced by $\frac{1}{2}a_0(111)$ meet.

$$M_{\mathcal{C}}(x+L_\perp)\equiv -M_{\mathcal{C}}(x) \tag{2}$$

for the instantaneous order parameter profile $M_{\mathcal{C}}(x)=(1/A)\sum_{y,z}M_{\mathcal{C}}(x,y,z)$ of a configuration $\mathcal{C}$ and

$$P_{\mathcal{C}}(x+L_\perp)\equiv P_{\mathcal{C}}(x) \tag{3}$$

for the profile of other quantities like concentration, internal energy, etc. ($A=\frac{1}{4}L_\parallel^2$ is the cross-section area.) The "interface position" $\bar{h}$ may then be defined by (a)

$$\left|\sum_{-(L_\perp-1)/2}^{(L_\perp-1)/2}M_{\mathcal{C}}(x+\bar{h}_a)\right|=\min\ \ (\approx 0) \tag{4}$$

or (b)

$$\left|\sum_{0}^{L_\perp-1}M_{\mathcal{C}}(x+\bar{h}_b)\right|=\max\ . \tag{5}$$

Summation extends over the x coordinate perpendicular to the interface.

In systems with very big cross-section area A, $M_{\mathcal{C}}(x)$ will be smooth and antisymmetric with respect to $\bar{h}$, and both definitions will yield the same value. The physical meaning of these definitions is verified by, e.g., assuming a hyperbolic tangent profile $M_{\mathcal{C}}(x)=M_{\text{bulk}}\tanh[(h-\bar{h}_{\mathcal{C}})/l_{\mathcal{C}}]$, $\bar{h}_{\mathcal{C}}$ being the position of the interface in configuration $\mathcal{C}$ and $l_{\mathcal{C}}$ the associated interface width. Both definitions then yield $\bar{h}_a=\bar{h}_b=\bar{h}_{\mathcal{C}}$. More generally,

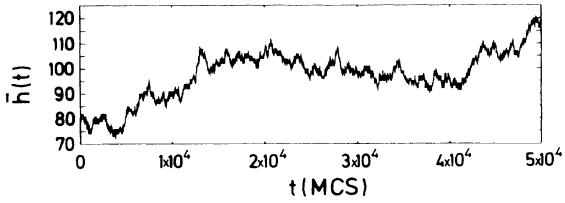

FIG. 3. Fluctuation of the interface position $\bar{h}(t)$ during the Monte Carlo simulation at $T/T_c=0.85$, $H=4|V_1|$, system size $L_\perp=159$, $L_\parallel=40$. Time t is measured in units of Monte Carlo steps per site (MCS), lengths are measured in units of half the lattice spacing $a_0/2$.

one gets an intuitive understanding of those definitions if one considers a solid-on-solid (SOS) model.[2] There $\bar{h}_a$ is simply the mean position of the interface and $\bar{h}_b$ gives the value of x where $M(x)$ passes zero.

The value $\bar{h}_b$ is most sensitive on changes of the order parameter profile in the direct neighborhood of the interface, whereas $\bar{h}_a$ also reacts on changes far away from it. Hence one would tend to prefer definition (b) at low temperatures, where the interface is well localized. However, because of finite size effects, definition (a) turns out to be more practical near T_c, as we will see. Actually we used both definitions and got the same results over nearly the whole range of temperatures. We will mainly show the results for definition (a) here.

Once the interface is localized in every configuration $\mathcal{C}$, one easily averages over profiles of quantities

$$P(x)=\langle P_{\mathcal{C}}(x+\bar{h}_{\mathcal{C}})\rangle \ . \tag{6}$$

$\langle\ \rangle$ means an average over configuration $\mathcal{C}$ that are analyzed in this way. We will now discuss the finite size effects related to this averaging procedure. In order to provide a qualitative understanding of the finite size effects that should be expected, we first construct a simple interface model.

(1) The interface itself has neither overhangs nor bubbles and may be described by a function $h(y,z)$ (SOS model).

(2) Quantities have local intrinsic profiles $P_{\text{intr}}(x)$ with respect to local interface position.

(3) The fluctuations $\eta(x,y,z)$ are the same in the bulk and at the interface. They show Ornstein-Zernicke behavior.

The order parameter in a configuration $\mathcal{C}$ is then given by

$$M_{\mathcal{C}}(x,y,z)=M_{\text{intr}}[x-h(y,z)]+\eta_{\mathcal{C}}(x,y,z) \ . \tag{7}$$

Let us first consider the case where local fluctuations can be neglected. Using the two procedures mentioned above, one gets the reference points h_a^0 and h_b^0 as well as the "ideal profiles" (index zero means that no fluctuations are included)

$$M_0(x)=\int dh\, M_{\text{intr}}(x-y) f_{a,b}(h) \ , \tag{8}$$

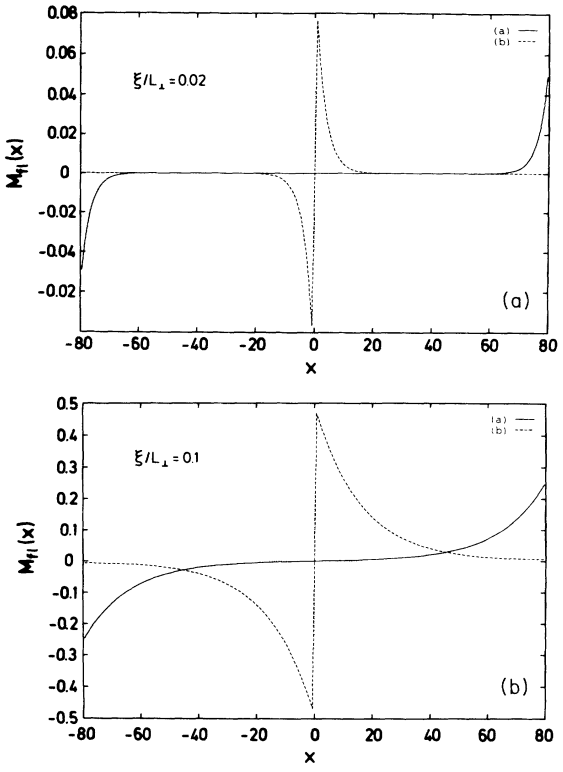

FIG. 4. Fluctuation-induced deviations from ideal profiles.

where $f_{a,b}(x)$ is the distribution function of the local interface position

$$f_{a,b}(x-h_{a,b}^0)=\langle \delta(x-[h(y,z)-h_{a,b}^0])\rangle \ . \tag{9}$$

Note that $f_{a,b}(x)$ may still depend on the system size; e.g., within the capillary wave approximation, f_a is Gaussian with a width increasing logarithmically with $L_\parallel$ [cf. Eq. (21)].

Fluctuations change the reference points $\bar{h}_a$ and $\bar{h}_b$ of a configuration and thus affect the averaged profiles. The calculation of these effects is carried out in Appendix A. One gets in case (a)

$$M(x)=M_0(x)+\frac{C}{L_\parallel^2}\left\{\frac{1}{2}M_0''(x)\frac{1}{M_{0,\text{bulk}}^2}\xi^2\left[\frac{1}{8}-\frac{\xi}{4L_\perp}\tanh\left[\frac{L_\perp}{2\xi}\right]\right]\right.$$
$$\left.+\sum_{n\geq 0,\text{odd}}\sin\left[\frac{\pi}{L_\perp}nx\right]\frac{1}{(\pi n)^2+(L_\perp/\xi)^2}(-1)^{(n-1)/2}\frac{1}{M_{0,\text{bulk}}}\right\} \tag{10}$$

and in case (b)

$$M(x)=M_0(x)+\frac{C}{L_\parallel^2}\left[\frac{1}{2}M_0''(x)\frac{1}{M_0'(0)^2}\frac{\xi}{4L_\perp}\tanh\left[\frac{L_\perp}{2\xi}\right]+\sum_{n\geq 0,\text{odd}}\sin\left[\frac{\pi}{L_\perp}nx\right]\right.$$
$$\left.\times\frac{1}{(\pi n)^2+(L_\perp/\xi)^2}\frac{1}{M_0'(0)}\frac{\pi n}{L_\perp}\right] , \tag{11}$$

where C is an amplitude measuring the strength of the fluctuations and ξ is the bulk correlation length in the direction normal to the interface. The effect of the second correction term is illustrated in Fig. 4 for different correlation lengths ξ. Close to T_c, the way (a) of localizing the interface obviously gives more reasonable results, because the largest deviations occur far away from the interface, whereas with procedure (b) they concentrate at the interface. Due to the numerous approximations made Eqs. (10) and (11) of course give qualitative descriptions of the expected finite size behavior only. But the actual simulation data indeed suggest that Eqs. (10) and (11) are useful.

Figure 5 shows profiles from simulations at tempera-

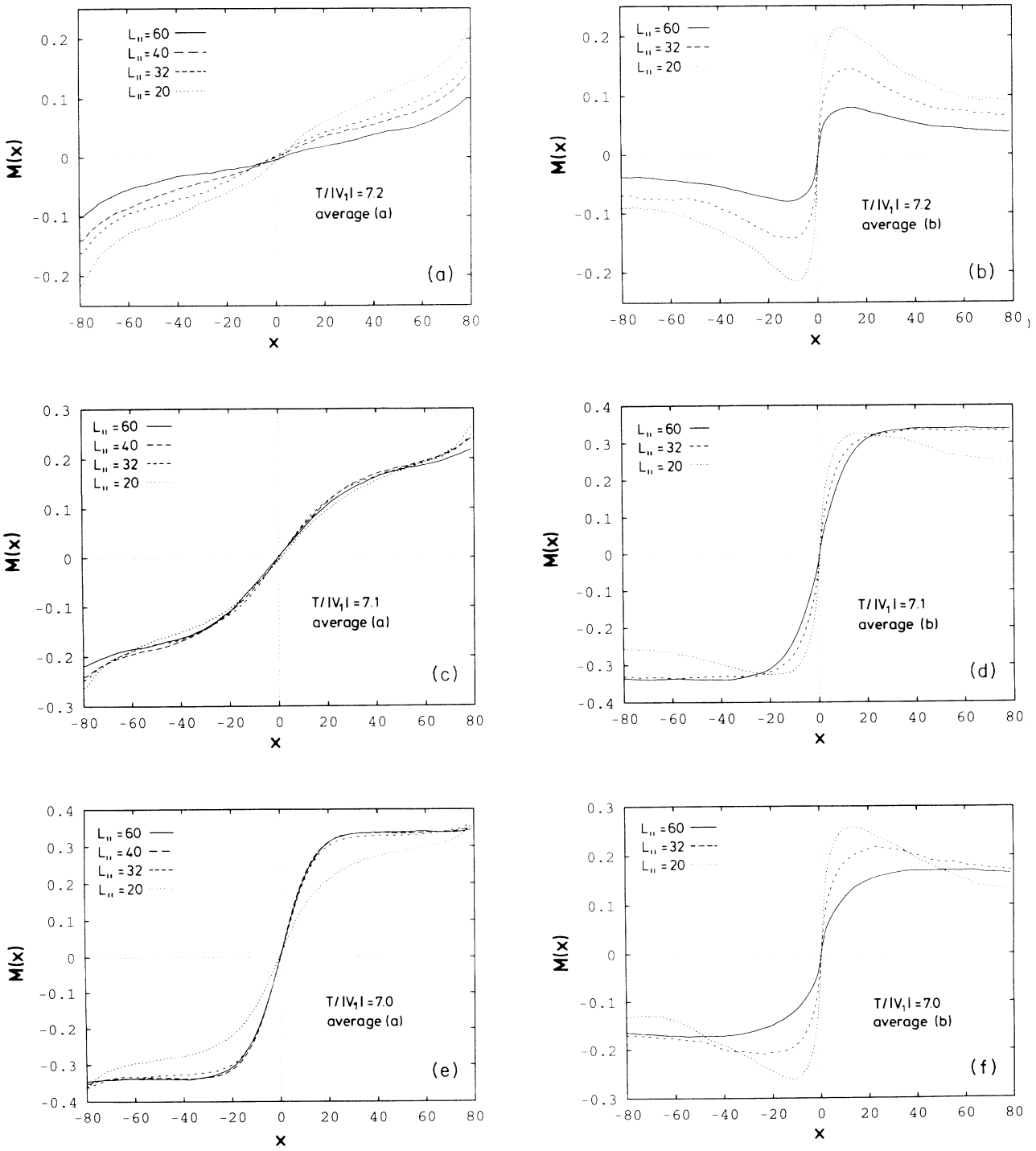

FIG. 5. Profiles averaged according to the prescription (a) or (b) at the temperature $T/|V_1|=7.2$, (a) and (b); at $T_c/|V_1|=7.1$, (c) and (d); and at $T/|V_1|=7.0$, (e) and (f). System linear dimension $L_{\text{perp}}=159$. Several choices of L_{parallel} are shown as indicated in the figure.

tures very close to T_c. One recognizes the structure of Fig. 4. The profiles slowly converge to a unique shape with increasing system size $L_\parallel$ as expected.

III. THEORETICAL CONSIDERATIONS

Generally the Landau expansion for the system near the second-order transition from the $B2$ phase to the $A2$ phase is given by

$$F=\int d^3r\left[\frac{A}{2}M^2(\mathbf{r})+\frac{B}{4}M^4(\mathbf{r})+\frac{C}{2}(\nabla M)^2+F_0-\mu c(\mathbf{r})\right], \tag{12}$$

where A, B, C, and F_0 will depend on the concentration $c(\mathbf{r})$ of negative Ising spins and on the temperature, and μ is a chemical potential. As is well known, in the bulk of the system this expression reduces to

$$F=F_0+\frac{A}{2}M^2+\frac{B}{4}M^4-\mu c \tag{13}$$

and the extrema of the free energy are given by $M=0$ (disordered phase, unstable) and $M=\pm M_{\text{bulk}}=\pm\sqrt{-A/B}$ (ordered phase, minimum) at temperatures below T_c [$A\propto(T-T_c)<0$]. The corresponding concentrations follow implicitly from the equations $\mu=(\partial/\partial c)(F_0-A^2/4B)|_{c_{\text{ord}}}$ in the ordered phase and $\mu=(\partial/\partial c)F_0|_{c_{\text{dis}}}$ in the disordered phase. Near the critical point we may expand $(\partial/\partial c)F_0|_{c_{\text{dis}}}\approx(\partial/\partial c)F_0|_{c_{\text{ord}}}+(c_{\text{dis}}-c_{\text{ord}})(\partial^2/\partial c^2)F_0|_{c_{\text{ord}}}$ neglecting higher-order terms. As we consider both ordered and disordered phases in the grand canonical ensemble at the same given chemical potential, we thus have to leading order $(c_{\text{dis}}-c_{\text{ord}})(\partial^2/\partial c^2)F_0|_{c_{\text{ord}}}=-(\partial/\partial c)(A^2/4B)|_{c_{\text{ord}}}$. Therefore the difference between the two concentrations behaves as

$$c_{\text{dis}}-c_{\text{ord}}=-\left[\frac{\partial}{\partial c}\frac{A^2}{4B}\right]_{c_{\text{ord}}}\left[\frac{\partial^2F_0}{\partial c^2}\right]^{-1}_{c_{\text{ord}}}\propto(T_c-T)\ . \tag{14}$$

Here we took into account that T_c varies linearly with concentration for the cases of interest.

At the interface one has to consider variations of the order parameter in one direction, $M=M(x)$, $c=c(x)$, and boundary conditions $M(\pm\infty)=\pm M_{\text{bulk}}$. If one assumes the variation $\delta c(x)$ of the concentration to be small, and therefore A, B, and C to be constant to first order, the minimization of F with respect to $M(x)$ yields an order parameter profile

$$M(x)=M_{\text{bulk}}\tanh(x/2\xi) \tag{15}$$

with the correlation length $\xi=\sqrt{-C/2A}$.[9]

The corresponding concentration profile in this approximation follows then as the solution of the equation

$$\mu=\frac{\partial}{\partial c}\left\{\frac{A}{2}M^2(x)+\frac{B}{4}M^4(x)+\frac{C}{2}\left[\frac{d}{dx}M(x)\right]^2+F_0\right\}. \tag{16}$$

As we are interested in interface segregation, we compute the deviation of the concentration at $M(x)=0$ and $x=0$, respectively. There one has to solve

$$\frac{\partial}{\partial c}\left[\frac{C}{2}\left[\frac{d}{dx}M\right]^2+F_0\right]\Bigg|_{x=0}=\mu\ . \tag{17}$$

After inserting $M(x)$ from Eq. (15) this leads to

$$\mu=\frac{\partial}{\partial c}(A^2/4B+F_0)|_{c=c(0)}\ . \tag{18}$$

One now expands μ again at $c=c_{\text{ord}}$ and gets

$$c(0)-c_{\text{ord}}=(c_{\text{dis}}-c_{\text{ord}})\frac{(\partial^2/\partial c^2)(2F_0)_{c_{\text{ord}}}}{(\partial^2/\partial c^2)(F_0+A^2/4B)_{c_{\text{ord}}}}\propto(T_c-T)\ . \tag{19}$$

Provided $A^2/B\propto(T_c-T)^2$ varies with concentration, the Landau theory thus predicts a segregation effect. Of course, the critical exponent ($\zeta=1$) predicted by Eqs. (14) and (19) is a mean-field result and hence not reliable.

The Landau theory naturally fails in describing the interface especially when it is rough. In this case the capillary wave approximation will be a more adequate approach.[10] We now recall some of its main features: The capillary wave model is a SOS model and starts from assuming that on the scale of the bulk correlation length ξ, the effective energy of an interface is proportional to the interface area. This leads to the Hamiltonian

$$\mathcal{H}=\frac{\sigma}{2}\sum_{q_{\min}\sim 1/\xi}^{q_{\max}\sim 1/L_\parallel}\tilde{h}(\mathbf{q})\tilde{h}(-\mathbf{q})q^2\ , \tag{20}$$

where $\tilde{h}$ is the Fourier transform of the interface position $h(y,z)$. The Fourier component $q=0$ is usually omitted in the sum. This corresponds to fixing a reference point (a) [Eq. (5)]. h is Gaussian distributed

$$f(x)=\langle\delta(h(y,z)-x)\rangle=\frac{1}{\sqrt{2\pi}w}e^{-h^2/2w^2} \tag{21}$$

with Gaussian width

$$w^2\propto\ln(L_\parallel/\xi)\ , \tag{22}$$

which depends on the extension $L_\parallel$ of the system in y,z direction. Thus one gets an order parameter profile

$$M(x)=M_{\text{bulk}}\int dh\ \theta(x-h)f(h)=M_{\text{bulk}}\,\text{erf}(x/\sqrt{2}w)\ . \tag{23}$$

Note that via the logarithmic dependence of w on $L_\parallel$ $M(x)$ also depends on $L_\parallel$.

IV. SIMULATION DATA

We did our simulations at $H/|V_1|=4$ in a temperature range of $T/|V_1|=1.5$ to $T/|V_1|=T_c/|V_1|=7.1$. The system size perpendicular to the interface was kept constant and very large ($L_\perp=159$), so that we could neglect corresponding finite size effects up to a temperature of $T/|V_1|=6.9$. This was checked by partially comparing

with even larger systems ($L_\perp = 239$). We only varied the system size parallel to the interface $L_\parallel = 20, 30, 40, 60$, thus simulating systems with 16 000–144 000 spins.

Figure 6 shows a typical order parameter profile. Apparently its shape might as well be described by a hyperbolic tangent as by an error function. However, the profile weakly, but clearly, broadens with increasing system size. The corresponding concentration profile exhibits an obvious segregation effect (Fig. 7).

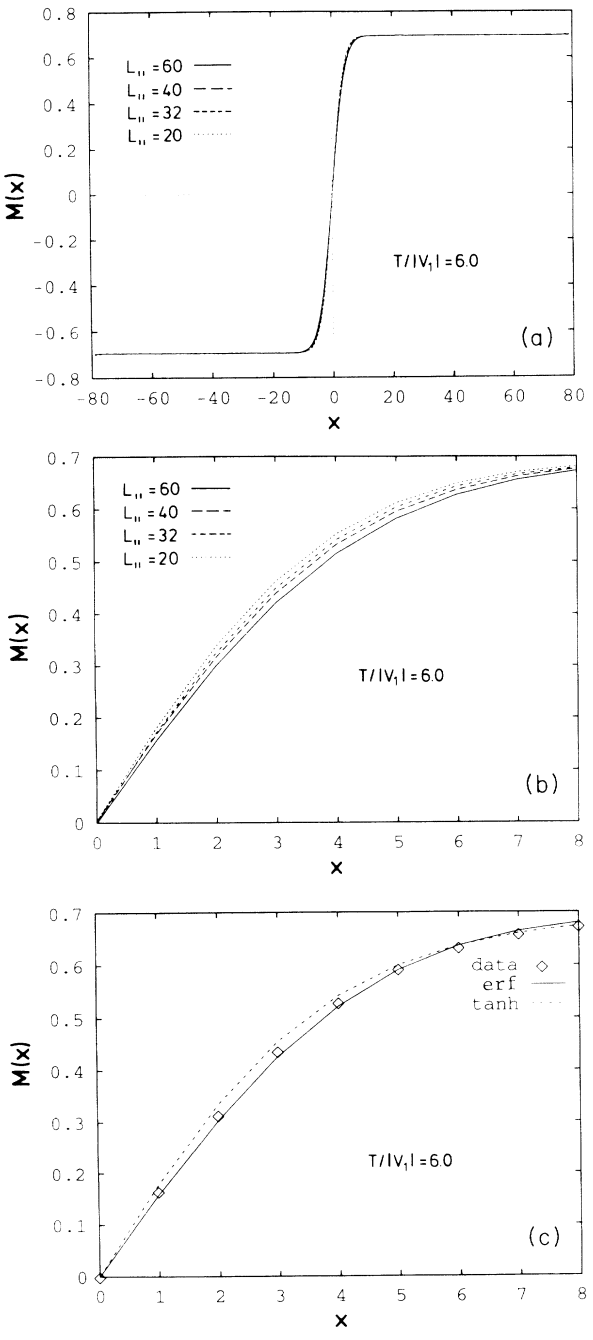

FIG. 6. (a) Order parameter profile at $T/|V_1| = 6$. Several choices $L_\parallel$ are shown as indicated in the figure. (b) Detail. (c) Fit of a hyperbolic tangent and an error function to the data at $L_\parallel = 40$.

The next step in analyzing the simulation data was to determine the profile width in a suitable way. We tried three possible definitions:

(a) the second moment of the order parameter profile

$$W_2^2 = \sum_{-L_\perp/2}^{L_\perp/2} F(x)x^2 - \left[\sum_{-L_\perp/2}^{L_\perp/2} F(x)x \right]^2 , \tag{24}$$

with

$$F(x) = \frac{1}{2M_{\text{bulk}}} [M(x) - M(x-1)] , \tag{25}$$

(b) the relative excess of the order parameter at the interface

$$W_M = \left| \frac{1}{M_{\text{bulk}}} \sum_{0}^{L_\perp - 1} [M(x) - M_{\text{bulk}}] \right| , \tag{26}$$

and (c) the relative excess of the concentration

$$W_c = \frac{1}{c(0) - c_{\text{bulk}}} \sum_{0}^{L_\perp - 1} [c(x) - c_{\text{bulk}}] . \tag{27}$$

In all three cases we qualitatively got the same results.

First of all the width clearly increases with the system length $L_\parallel$ down to the temperature $T/|V_1| \gtrsim 3$ and the

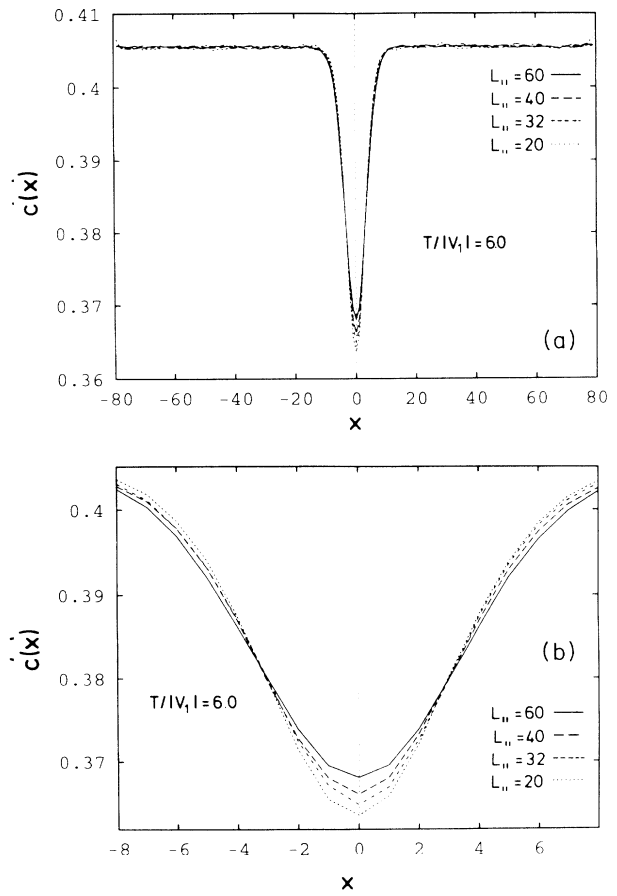

FIG. 7. (a) Concentration profile $c(x)$ of spins "−1" at $T/|V_1| = 6$. (b) Detail.

data can very well be fitted to a logarithmic law

$$W^2 = a^2 \ln(L/s) \tag{28}$$

(Fig. 8). One now can extract the two characteristic lengths a and s for each temperature. For comparison we also determined the bulk correlation length ξ, defined by

$$\xi^2 = \frac{1}{3}\frac{\int x^4 \Gamma(x)dx}{\int x^2 \Gamma(x)dx} , \tag{29}$$

where $\Gamma(x)$ is the bulk correlation function

$$\Gamma(x) = \langle M(x)M(0)\rangle - \langle M\rangle^2 . \tag{30}$$

[At low temperatures ξ is expected to depend on the direction in the lattice.[11] As we are interested in the correlation length in the direction normal to the interface mainly, we inserted the bulk correlation function $\Gamma(x)$ in cubic directions (100) here. To determine it we did simulations on cubic bulk systems with 8192 and 16 000 spins.] The results are shown in Fig. 9. The bulk correlation length clearly shows the expected behavior $\xi \propto |T_c - T|^{-\nu}$ with $\nu = 0.63$, and a and s follow the same power law. Obviously the correlation length also remains the only relevant length scale at the interface as is the case in the bulk.

To finish the discussion of the profile widths we compare the width extracted from the excess of the order parameter (b) and from the excess of the concentration (c). In a pure SOS model the local order parameter follows a step function at the interface and the local concentration has a sharp maximum. This would lead to

$$\frac{W_M}{W_c} = 2\langle |h| \rangle_f f(0) , \tag{31}$$

where f is the distribution function of the interface position $h(y,z)$ (see Appendix B). The capillary wave approximation then yields [Eq. (21)]

$$\frac{W_c}{W_M} = \frac{\pi}{2} . \tag{32}$$

With this result another independent check of the theory is available. Figure 10 shows that the capillary wave approximation seems to be valid at temperatures higher than $T/|V_1| \gtrsim 4$. However, there still remains a small systematic deviation of about 3%. It depends neither on the system size, nor on the temperature—therefore one cannot explain this effect simply by the fact that a lattice model has been described by a continuous theory.

Next we will have a closer look at the phenomenon of interface segregation. As Figs. 7 and 11 illustrate, there is a clear enrichment of spins "+1" at the interface. Qualitatively this can be understood quite easily: The $B2$ ordering favors equal concentration of both atom types On the other hand, at $H = 4$, one would expect a higher concentration of spins +1 in a disordered system. The interface resembles a disordered layer, therefore spins +1 will accumulate there.

The critical exponent of the segregation can be deduced by a simple analysis of scaling dimensions.[12] The chemical potential H has the same scaling dimension as the temperature, hence the scaling dimension of the concentration is $-[H]-d = 1/\nu - d$. Therefore the segregated concentration scales like

$$c_{\text{segr}} = c_{\text{extr}} - c_{\text{bulk}} \propto (T_c - T)^{\zeta} \tag{33}$$

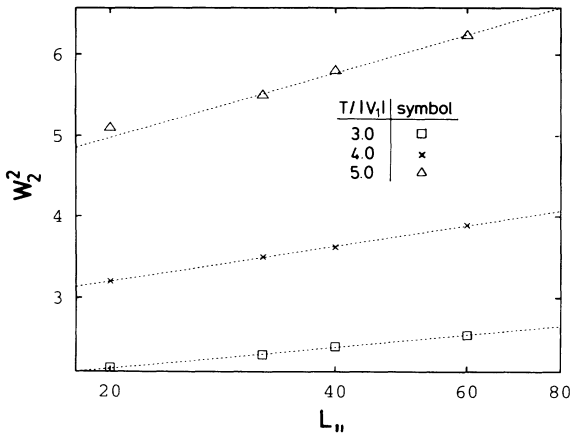

FIG. 8. W_2^2 vs $L_\parallel$ for different temperatures as indicated in the figure. Straight lines are fits of the function $a^2 \ln(L/s)$ to the data points corresponding to the three larger system sizes.

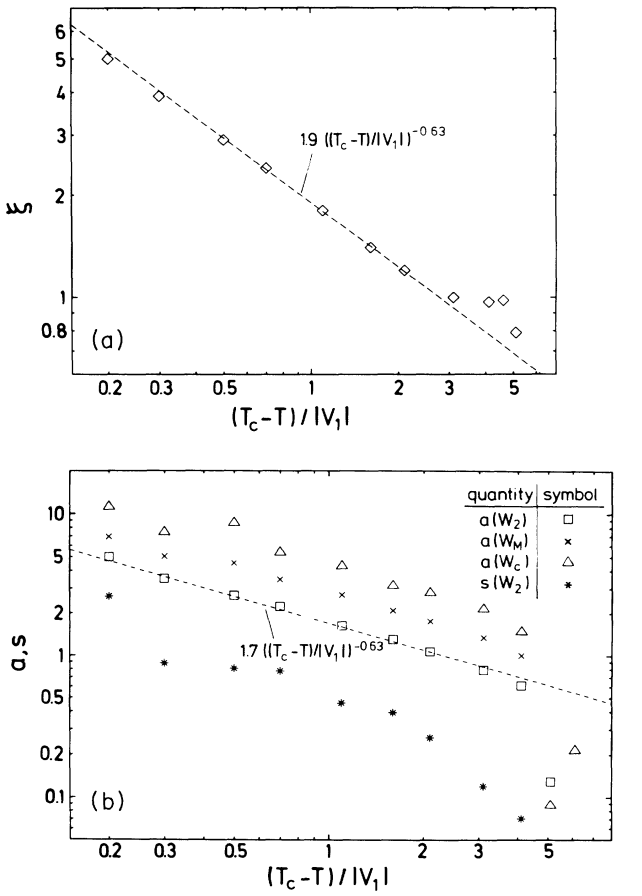

FIG. 9. (a) Bulk correlation length at $H/|V_1| = 4$. (b) a and s vs temperature (explanation in the text). The data for s extracted from the size dependence of W_M and W_c are similar.

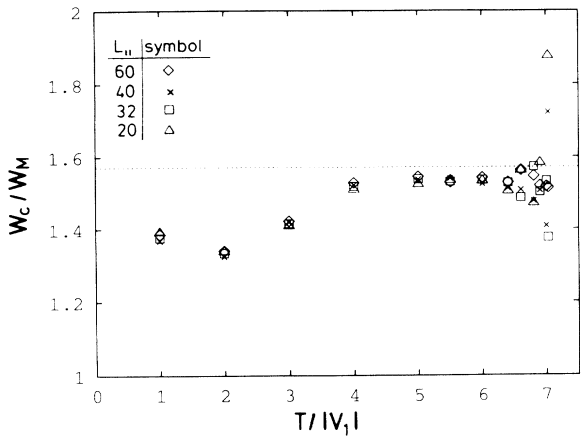

FIG. 10. Comparison of relative order parameter excess and relative concentration excess at the interface as function of temperature.

with $\zeta=(1/\nu-d)(-\nu)=1-\alpha$. In the Landau theory we recover $\zeta=1$, while in the three-dimensional Ising model we get $\zeta=0.89$. Figure 12 demonstrates that our simulation data scale very well with $\zeta=0.89$ and a bit worse with $\zeta=1$.

At the end of this section we consider the scaling properties of excess quantities. Let y be the critical exponent and $d_A=-y/\nu$ the scaling dimension of the density of an extensive quantity A. The excess of A, defined as

$$A_{\text{exc}}=\int [A(x)-A_{\text{bulk}}]dx \ , \tag{34}$$

has the scaling dimension d_A+1 and thus the critical exponent $\tilde{\omega}=y-\nu$. The excess of the order parameter, e.g., should scale with the exponent $\tilde{\omega}=\beta-\nu=-0.31$, for the excess of the concentration one gets $\tilde{\omega}=\zeta-\nu=0.26$, and the interface free energy[13] follows the power law

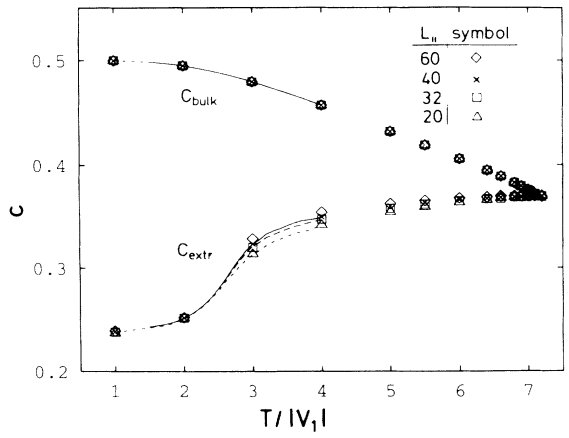

FIG. 11. Extreme value of the concentration of negative Ising spins at the interface c_{extr} compared with the bulk value c_{bulk} as function of temperature.

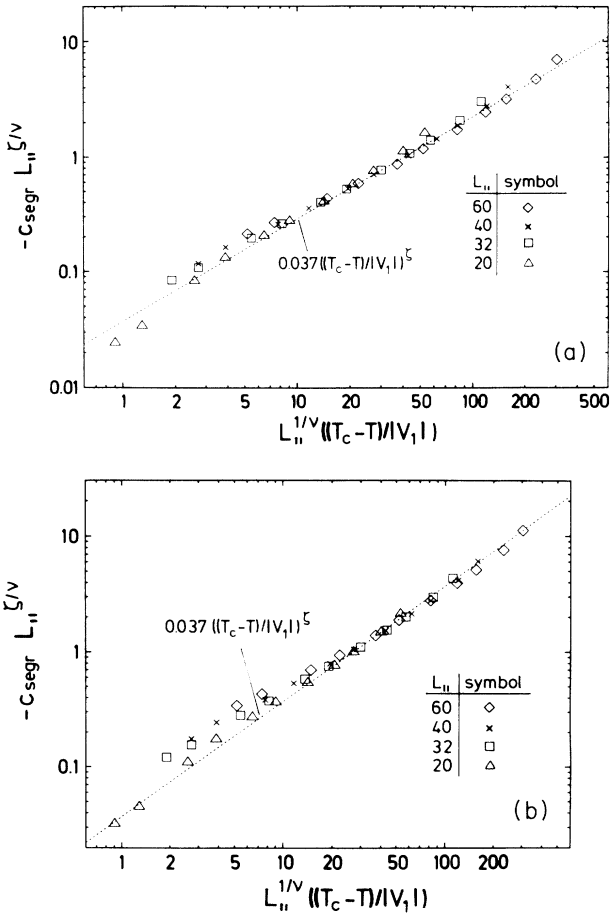

FIG. 12. Finite size scaling plot of the segregated concentration c_{segr} with (a) $\zeta=0.89$, (b) $\zeta=1$ (see Ref. 16 for the theory of finite size scaling).

$$f\propto(T_c-T)^{\mu} \quad \text{with } \mu=(d-1)\nu=1.26 \tag{35}$$

(see also Ref. 14 for similar considerations). The comparison with Figs. 13–15 shows that this concept describes the simulation data in a satisfactory way.

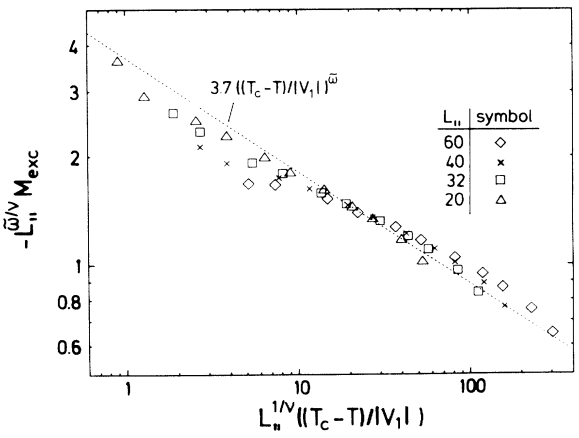

FIG. 13. Finite size scaling plot of the excess of the order parameter, scaled with $\tilde{\omega}=-0.31$.

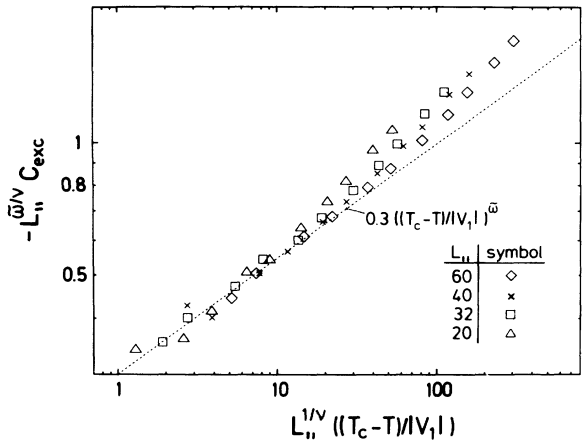

FIG. 14. Finite size scaling plot of the excess of the concentration, scaled with $\bar{\omega}=0.26$.

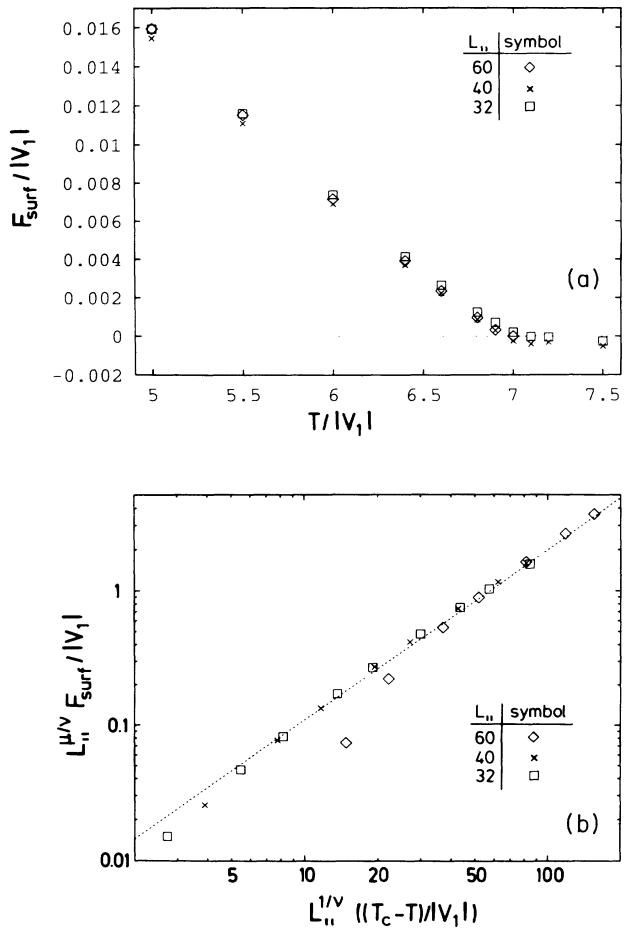

FIG. 15. Interfacial free energy plotted vs temperature, (a) raw data and (b) scaled with $\mu=1.26$. F_{surf} was determined by computing the free energy of a system with and without an interface via thermodynamic integration (Ref. 17) and subtracting them from each other.

V. SUMMARY AND OUTLOOK

In this paper we have presented simulation results for interfaces in a complex system. As we worked with periodic boundary conditions, we had no border effects and could deal with rather small systems even close to T_c. However, since we had imposed translational invariance to the system, the evaluation of averaged profiles required a special analysis procedure. We have developed such a procedure, analyzed corresponding finite size effects, and shown that it offers a suitable way of handling the simulation data.

Our interface turned out to be rough over nearly the whole range of temperatures. We have seen that at temperatures not too close to the roughening temperature $T_R/|V_1|=2.7$ (the results connected with the roughening transition will be presented in Ref. 15) the data are well described by the capillary wave approximation, except for a small systematic deviation of $\sim 3\%$.

By extracting the different lengths associated to the width of the interface and comparing them with the bulk correlation length, we have shown that near T_c the interface does not introduce a new length scale into the system. Thus we confirm the result of an earlier investigation in an Ising system, where, however, the interface roughness and therefore the dependence of the interface width on the system size has not been taken into account.[18] We found that particularly the degree of roughness of the interface is determined only by the correlation length. As a consequence one expects all quantities to exhibit standard finite size scaling behavior. Our data reproduced this nicely.

As another important result we have shown that interfacial segregation occurs even in a lattice model, despite the lack of mechanical strains and forces. The phenomenon of segregation is connected to the fact that the stoichiometry of the bulk deviates from the stoichiometry in the ideally ordered phase (in the $B2$ phase 1:1): The deviation is amplified at the interface.

Thus we have seen that the Monte Carlo study of interfaces, especially of profiles of diverse quantities in the neighborhood of interfaces, is feasible even in such a complex system, and yields a variety of interesting phenomena. Of course, there still remain many interesting questions that could be tackled now. One could investigate the behavior of the interface near a first-order transition, hence comparing the present model with the model of a fcc crystal discussed in Ref. 5. Furthermore, it would be interesting to see how things change in the neighborhood of a multicritical point. We have not seen an oscillatory concentration profile as it has, e.g., been measured recently in an internal interface in Pt(Ni).[4] But perhaps other interfaces in the system exhibit such a behavior. As another step in order to improve the model one could include vacancies. Then the modeling of interfaces becomes much more realistic, because vacancies play a crucial role especially in connection with segregation.

We conclude that internal interfaces in crystals still represent a challenging research field with many problems waiting to be solved. We hope that our work will stimulate theoretical effort to understand why the capil-

lary wave theory is not entirely successful in describing the simulation data, as well as similar numerical studies on other interfaces. Furthermore it would of course be most revealing if experimental investigations of the temperature-dependent structure of antiphase boundaries in iron-aluminum were available that could be compared directly with our simulation data.

ACKNOWLEDGMENTS

One of us (F.S.) received support from the Landesgraduierten-Förderungsgesetz Rheinland-Pfalz. F.S. wishes to thank J. Baschnagel for fruitful discussions. This work was carried out using extensive computer time at the Siemens-Fujitsu VP100 computer at the Regionales Hochschulrechenzentrum Kaiserslautern (RHRK) and at the Cray YMP at the Höchstleistungsrechenzentrum Jülich (HLRZ).

APPENDIX A

We start from the order parameter profile of a configuration $\mathcal{C}$,

$$M_{\mathcal{C}}(x+h^0_{a,b})=\frac{1}{A}\int dy\,dz\,M_{\rm intr}[x-\tilde{h}_{a,b}(y,z)]+\tilde{\eta}_{\mathcal{C}}(x)\ , \tag{A1}$$

where

$$\tilde{h}_{a,b}(y,z)=h(y,z)-h^0_{a,b}$$

and

$$\tilde{\eta}_{\mathcal{C}}(x)=\frac{1}{A}\int dy\,dz\,\eta_{\mathcal{C}}(x+h^0_{a,b},y,z)\ .$$

$h^0_{a,b}$ are reference points for a system without fluctuations, as they have been introduced in the text. Note that the fluctuations are averaged over the cross-section area A, hence the effect they produce will be smaller, the larger $A\propto L_\parallel^2$ is:

$$\langle\tilde{\eta}^2\rangle\propto\frac{1}{L_\parallel^2}\langle\eta^2\rangle\ . \tag{A2}$$

Like $M_{\mathcal{C}}$, $\tilde{\eta}_{\mathcal{C}}(x)$ is periodic with the period $2L_\perp$. Therefore it can be expanded into a Fourier series:

$$\tilde{\eta}_{\mathcal{C}}(x)=\sum_n e^{i(\pi/L_\perp)nx}c_{n,\mathcal{C}}\ , \tag{A3}$$

where

$$c_{n,\mathcal{C}}=c^*_{-n,\mathcal{C}}\quad(\tilde{\eta}\text{ is real})\ ,$$

$$\langle c_{n,\mathcal{C}}\rangle_{\mathcal{C}}=0\quad(\langle\tilde{\eta}\rangle=0)\ ,$$

$$c_{n,\mathcal{C}}=0\quad\text{for even } n\quad[\tilde{\eta}_{\mathcal{C}}(x)=-\tilde{\eta}_{\mathcal{C}}(x\pm L_\perp)]\ .$$

This leads to a Fourier series in sine/cosine functions

$$\tilde{\eta}_{\mathcal{C}}(x)=\sum_{n\ge0}\left[a_{n,\mathcal{C}}\sin\left[\frac{\pi}{L_\perp}nx\right]+b_{n,\mathcal{C}}\cos\left[\frac{\pi}{L_\perp}nx\right]\right]\ , \tag{A4}$$

with

$$a_{n,\mathcal{C}}=-2\,\mathrm{Im}(c_{n,\mathcal{C}}),\quad b_{n,\mathcal{C}}=2\,\mathrm{Re}(c_{n,\mathcal{C}})\ .$$

If one takes into consideration these fluctuations the reference point $h_{a,b}=h^0_{a,b}+\delta h_{a,b}$ will shift in the following way.

(a) δh_a is defined by

$$\int_{-L_\perp/2}^{L_\perp/2}M_{\mathcal{C}}(x+h^0_a+\delta h_a)dx=0\ . \tag{A5}$$

Since

$$\int_{-L_\perp/2}^{L_\perp/2}dx\frac{1}{A}\int dy\,dz\,M_{\rm intr}[x-\tilde{h}_a(\mathbf{o})]=0\ , \tag{A6}$$

Eqs. (A1) and (A3) lead to

$$\int_{L_\perp/2-\delta h_a}^{L_\perp/2+\delta h_a}dx\frac{1}{A}\int dy\,dz\,M_{\rm intr}[x-\tilde{h}_a(y,z)]+2\sum_n e^{i[(\pi/L_\perp)n\delta h_a]}(-1)^{(n-1)/2}\frac{L_\perp}{\pi n}c_{n,\mathcal{C}}=0\ .$$

Let finite size effects be so small that they can be disregarded to second order. Expanding the above equation linearly in δh_a, one gets

$$\frac{1}{A}\int dy\,dz\,M_{\rm intr}\left[\frac{L_\perp}{2}-\tilde{h}_a(y,z)\right]\delta h_a+\sum_n(-1)^{(n-1)/2}\frac{L_\perp}{\pi n}c_{n,\mathcal{C}}=0\ .$$

For large enough $L_\perp$ the integral far away from the interface position simply yields the bulk value of the order parameter,

$$\frac{1}{A}\int dy\,dz\,M_{\rm intr}\left[\frac{L_\perp}{2}-\tilde{h}_a(y,z)\right]=M_{0,\rm bulk}\ ,$$

hence one has

$$\delta h_a=\frac{1}{M_{0,\rm bulk}}\sum_{n\ge0,\rm odd}(-1)^{(n+1)/2}\frac{L_\perp}{\pi n}b_{n,\mathcal{C}}\ . \tag{A7}$$

(b) δh_b is determined by

$$\left|\int_0^{L_\perp}M_{\mathcal{C}}(x+h^0_b+\delta h_b)dx\right|=\max\ . \tag{A8}$$

As

$$I:=\left|\int_0^{L_\perp}dx\frac{1}{A}\int d^{d-1}o\,M_{\rm intr}[x-\tilde{h}_b(\mathbf{o})]\right|=\max \tag{A9}$$

is already fulfilled, (A1) and (A3) lead to

$$\left|I-2\int_0^{\delta h_b}dx\frac{1}{A}\int dy\,dz\,M_{\rm intr}[x-\tilde{h}_b(\mathbf{o})]+2\sum_n e^{i(\pi/L_\perp)n\delta h_b}\frac{iL_\perp}{\pi n}c_{n,\mathcal{C}}\right|=\max\ .$$

After having differentiated with respect to δh_b and neglecting higher orders of $\tilde{\eta}$ and δh_b, one gets

$$\frac{1}{A}\int dy\,dz\,M_{\rm intr}[\delta h_b-\tilde{h}_b(\mathbf{o})]+\sum_n c_{n,\mathcal{C}}=0\ .$$

Finally one expands the intrinsic profile in powers of δh_b.

$$\frac{1}{A}\int dy\,dz\,M_{\rm intr}[\delta h_b-\tilde{h}_b(\mathbf{o})]$$

$$\approx\frac{1}{A}\int dy\,dz\{M_{\rm intr}[-\tilde{h}_b(\mathbf{o})]+\delta h_b M'_{\rm intr}[-\tilde{h}_b(\mathbf{o})]\}\ .$$

In a system without fluctuations δh_b^0 should give zero, therefore one has

$$\frac{1}{A}\int dy\,dz\,M_{\rm intr}[-\tilde{h}_b(\mathbf{o})]=0 \tag{A10}$$

and

$$\delta h_b=-\frac{1}{M'_0(0)}\sum_{n\geq 0,\rm odd} b_{n,\mathcal{C}}\ . \tag{A11}$$

$M'_0(0)$ is defined as $(d/dx)M_0(x)|_{x=0}$.

Let us now assume that the Fourier components of the fluctuations do not couple to each other.

$$\langle a_{n,\mathcal{C}}b_{m,\mathcal{C}}\rangle=0\ ,\quad \langle a_{n,\mathcal{C}}a_{m,\mathcal{C}}\rangle=\langle b_{n,\mathcal{C}}b_{m,\mathcal{C}}\rangle=\delta_{nm}f_n\ . \tag{A12}$$

The averaged order parameter profile is given by

$$M(x)=\left\langle\frac{1}{A}\int dy\,dz\,M_{\rm intr}[x-\tilde{h}_{a,b}(y,z)+\delta h_{a,b}]\right\rangle + \langle\tilde{\eta}_{\mathcal{C}}(x+\delta h_{a,b})\rangle\ . \tag{A13}$$

The right-hand side of this equation can be expanded in powers of $\delta h_{a,b}$. As $b_{n,\mathcal{C}}$ does not depend on the concrete structure of the interface $\{\tilde{h}(y,z)\}$, the first term gives

$$\left\langle\frac{1}{A}\int dy\,dz\,M_{\rm intr}[x-\tilde{h}_{a,b}(y,z)+\delta h_{a,b}]\right\rangle = M_0(x)+\tfrac{1}{2}M''_0(x)\langle\delta h_{a,b}^2\rangle+\cdots$$

with

$$\langle\delta h_a^2\rangle=\frac{1}{M_{0,\rm bulk}^2}\sum\left[\frac{L_\perp}{\pi n}\right]^2\langle b_{n,\mathcal{C}}^2\rangle\ , \tag{A14}$$

$$\langle\delta h_b^2\rangle=\frac{1}{M'_0(0)^2}\sum\langle b_{n,\mathcal{C}}^2\rangle\propto\langle\tilde{\eta}^2\rangle \tag{A15}$$

and the second term [see Eq. (A4)]

$$\langle\tilde{\eta}_{\mathcal{C}}(x+\delta h_{a,b})\rangle=\sum\left[\cos\left[\frac{\pi}{L_\perp}nx\right]\left\langle a_n\frac{n\pi}{L_\perp}\delta h_{a,b}\right\rangle-\sin\left[\frac{\pi}{L_\perp}nx\right]\left\langle b_n\frac{n\pi}{L_\perp}\delta h_{a,b}\right\rangle\right]+\cdots$$

$$=\sum_{n\geq 0,\rm odd}\sum\sin\left[\frac{\pi}{L_\perp}nx\right]\langle b_n^2\rangle\begin{cases}\dfrac{1}{M_{0,\rm bulk}}(-1)^{(n-1)/2} & \text{(A16a)}\\[2ex] \dfrac{1}{M'_0(0)}\dfrac{n\pi}{L_\perp}\ . & \text{(A16b)}\end{cases}$$

At this point we have to put in the Ornstein-Zernicke behavior:

$$\langle a_{n,\mathcal{C}}^2\rangle=\langle b_{n,\mathcal{C}}^2\rangle=\frac{C}{L_\parallel^2}\frac{1}{L_\perp^2}\frac{1}{(\pi n/L_\perp)^2+(1/\xi)^2}\quad\text{for odd } n \tag{A17}$$

with the correlation length ξ and some amplitude C. Because of

$$\sum_1^\infty g_n=\frac{\pi}{4}a\tanh\left[\frac{\pi}{2a}\right]\ ,$$

where

$$g_n=\begin{cases}\dfrac{1}{n^2+a^{-2}} & \text{for odd } n\\ 0 & \text{for even } n\ ,\end{cases}$$

one has

$$\langle\delta h_a^2\rangle=\frac{C}{L_\parallel^2}\frac{1}{M_0^{\rm bulk^2}}\xi^2\left[\frac{1}{8}-\frac{\xi}{4L_\perp}\tanh\left[\frac{L_\perp}{2\xi}\right]\right]\ , \tag{A18}$$

$$\langle\delta h_b^2\rangle=\frac{C}{L_\parallel^2}\frac{1}{M'_0(0)^2}\frac{\xi}{4L_\perp}\tanh\left[\frac{L_\perp}{2\xi}\right]\ . \tag{A19}$$

This finally leads to Eqs. (10) and (11).

APPENDIX B

In the continuum limit, the width extracted from the excess of the order parameter is given by

$$W_M=\left|\frac{1}{M_{\rm bulk}}\int_0^{L_\perp}[M(x)-M_{\rm bulk}]dx\right|$$

$$=\frac{1}{M_{\rm bulk}}\left|\int_{-L_\perp/2}^{0}[M(x)+M_{\rm bulk}]dx-\int_0^{L_\perp/2}[M(x)-M_{\rm bulk}]dx\right|\ . \tag{B1}$$

Let $L_\perp$ go to infinity and the order parameter profile $M(x)$ satisfy the boundary conditions $M(-\infty)=-M_{\text{bulk}}$ and $M(+\infty)=+M_{\text{bulk}}$. $M(x)$ then depends on the interface distribution function $f(h)$ via

$$M(x)=M_{\text{bulk}}\int_{-\infty}^{\infty} dh\ \theta(x-h)f(h)\ . \tag{B2}$$

Because of $\int f(h)dh=1$ this leads to

$$W_M=\int_0^{\infty}dx\int_{-\infty}^{\infty}dh\ f(h)s(x,h)$$

$$\text{with } s(x,h)=2+\theta(-x-h)-\theta(x-h)\ . \tag{B3}$$

One easily checks $s(x,h)=2$ for $0<x<|h|$ and $s(x,h)=0$ for $x>|h|$. Thus one gets

$$W_M=2\int_{-\infty}^{\infty}dh\ f(h)\int_0^{|h|}dx=2\langle|h|\rangle_f\ . \tag{B4}$$

The width extracted from the excess of the concentration is

$$W_c=\frac{1}{c(0)-c_{\text{bulk}}}\int_0^{L_\perp}[c(x)-c_{\text{bulk}}]dx$$

$$=\frac{1}{c(0)-c_{\text{bulk}}}\int_{-L_\perp/2}^{L_\perp/2}[c(x)-c_{\text{bulk}}]dx\ . \tag{B5}$$

As the concentration profile $c(x)$ is connected with $f(h)$ through

$$c(x)-c_{\text{bulk}}=C_0f(x) \tag{B6}$$

(C_0 is some proportionality factor), this yields

$$W_c=\frac{1}{C_0f(0)}\int C_0f(x)dx=\frac{1}{f(0)}\ . \tag{B7}$$

In the capillary wave theory the distribution function is given by Eq. (21): $f(0)=1/(\sqrt{2\pi}w)$ and $\langle|h|\rangle_f=w\sqrt{2/\pi}$. Thus one gets $W_c/W_M=\pi/2$.

[1]See, for example, *Interfacial Aspects of Phase Transformations,* Vol. 76 of *NATO Advanced Study Institute, Series B: Physics,* edited by Boyan Mutaftschiev (Reidel, Dordrecht, 1982).

[2]For surveys, see S. Dietrich, in *Phase Transitions and Critical Phenomena,* edited by C. Domb and J. L. Lebowitz (Academic, New York, 1988), Vol. 12; G. Forgacs, R. Lipowsky, and Th. M. Niewenhuizen, *ibid.* (Academic, New York, 1991), Vol. 14.

[3]*Interfacial Segregation,* edited by W. C. Johnson and J. M. Blakely (American Society for Metals, Metals Park, OH, 1979).

[4]J. G. Hu and D. N. Seidman, Phys. Rev. Lett. **65**, 1615 (1990); S. M. Kuo, A. Seki, Y. Oh, and D. N. Seidman, *ibid.* **65**, 199 (1990); D. Udler, J. G. Hu, S. M. Kuo, A. Seki, B. W. Krakauer, and D. N. Seidman, Scr. Metall. Mater. **25**, 841 (1991).

[5]A. Finel, V. Mazauric, and F. Ducastelle, Phys. Rev. Lett. **65**, 1016 (1990); C. Leroux, A. Loiseau, M. C. Cadeville, D. Broddin, and G. van Tendeloo, J. Phys. Condens. Matter **2**, 3479 (1990); C. Leroux, A. Loiseau, M. C. Cadeville, and F. Ducastelle, Europhys. Lett. **12**, 155 (1990); A. Loiseau, C. Leroux, D. Broddin, and G. van Tendeloo, J. Phys. (Paris) Colloq. **51**, C1-223 (1990).

[6]R. Kikuchi and J. W. Cahn, Acta Metall. **27**, 1337 (1979).

[7]F. Schmid, and K. Binder, J. Phys. Condens. Matter **4**, 3569 (1992).

[8]V. Pierron-Bohnes, M. C. Cadeville, O. Schaerpf, and A. Finel, J. Phys. (Paris) **1**, 247 (1991).

[9]J. W. Cahn and J. E. Hilliard, J. Chem. Phys. **28**, 258 (1958).

[10]F. P. Buff, R. A. Lovett, and F. H. Stillinger, Phys. Rev. Lett. **15**, 621 (1965); J. D. Weeks, J. Chem. Phys. **67**, 3106 (1977); Phys. Rev. Lett. **52**, 2160 (1984); J. S. Rowlinson, and B. Widom, in *Molecular Theory of Capillarity* (Clarendon, Oxford, 1982); D. Bedeaux and J. D. Weeks, J. Chem. Phys. **82**, 972 (1985).

[11]H. B. Tarko and M. E. Fisher, Phys. Rev. B **11**, 1217 (1975).

[12]See, for example, S. Ma, *Modern Theory of Critical Phenomena,* Frontiers in Physics (Benjamin Cummings, Menlo Park, CA, 1976).

[13]B. Widom, J. Chem. Phys. **43**, 3892 (1965).

[14]W. Selke, Z. Phys. B **47**, 335 (1982); **50**, 113 (1983); W. Selke and J. Yeomans, J. Phys. A **16**, 2789 (1983).

[15]F. Schmid and K. Binder, following paper, Phys. Rev. B **46**, 13 572 (1992).

[16]M. N. Barber, in *Phase Transition and Critical Phenomena,* edited by C. Domb and J. L. Lebowitz (Academic, New York, 1983), Vol. 8.

[17]K. Binder, in *Monte Carlo Methods in Statistical Physics,* edited by K. Binder (Springer, Berlin, 1979).

[18]H. J. Leamy, G. H. Gilmer, K. A. Jackson, and P. Bennema, Phys. Rev. Lett. **30**, 601 (1973).